

Spin-fracton effects in dilute amorphous alloys

M. B. Salamon

Department of Physics and Materials Research Laboratory, University of Illinois at Urbana-Champaign,
1110 West Green Street, Urbana, Illinois 61801

Y. Yeshurun

Department of Physics, Bar Ilan University, 52100 Ramat-gan, Israel
(Received 4 November 1986; revised manuscript received 1 June 1987)

Deviations from the Bloch $T^{3/2}$ law, observed in dilute amorphous magnets, are shown to result from the crossover from magnon to fracton density of states. Data from a series of amorphous $(\text{Co}_p\text{Ni}_{1-p})_{75}\text{P}_{16}\text{B}_6\text{Al}_3$ alloys were fitted to an approximate density-of-states function that matches the two regimes at a frequency $\omega_c(p)$. Both the magnon stiffness constant and ω_c decrease as powers of $p - p_c$, where p_c is the percolation concentration. The exponents are consistent with a value of $\theta = 1.5$ used in the fracton density of states and in agreement with percolation theory.

Bloch's famous $T^{3/2}$ law¹ provided some of the earliest evidence for the existence of quantized spin waves in isotropic ferromagnets.¹ Since each spin excitation reduces the magnetization of the ferromagnet by one Bohr magneton, the well-known law²

$$M(T)/M(0) = 1 - BT^{3/2} \quad (1)$$

follows from a Bose-Einstein integration of

$$n_{sw}(\omega) = (1/4\pi^2)(\hbar/D)^{3/2}\omega^{1/2}, \quad (2)$$

the spin-wave density of states (DOS) per unit volume.² These results have been tested experimentally on many isotropic three-dimensional magnets. In dilute amorphous alloys, however, significant deviations from Bloch's law are observed and were recognized by Bhagat, Spano, Chen, and Rao³ to signal changes in the spin-wave DOS at a characteristic frequency ω_c . It is the purpose of this Brief Report to demonstrate that a crossover of the DOS from the spin-wave to the so-called⁴ "fracton" regime explains, in detail, those deviations from Bloch's law. We believe this to provide the clearest evidence to date⁵ for fractal excitation in diluted magnets.

Experimental data for $M(T)/M(0)$ are usually plotted versus $T^{3/2}$ in order to obtain B , and thus the stiffness constant D . The presence of higher-order terms in the dispersion relation and renormalization of D causes such plots to curve downward at high temperature.² An applied magnetic field induces a gap in the spin-wave dispersion curve and leads to downward curvature at low temperatures as well.² The deviations observed in dilute amorphous magnets manifest themselves in an upward-curving plot³ over a very wide temperature range, often spanning the Curie point. This effect becomes increasingly more pronounced as the concentration of the magnetic constituent is decreased. A set of such data is shown in Fig. 1 for the system $(\text{Co}_p\text{Ni}_{1-p})_{75}\text{P}_{16}\text{B}_6\text{Al}_3$. Nickel is nonmagnetic in this amorphous material. The present analysis supercedes our previous study⁶ of this system, in which disregard of the curvature led to results in disagreement with the prediction of percolation theory that the stiffness constant D should vanish as $T_C \rightarrow 0$

In a dilute magnet above the percolation point p_c , only those spin excitations with wavelengths longer⁷ than the percolation correlation length ξ_p have quadratic dispersion. The stiffness constant is a function of concentration,⁸ and is given by

$$D(p) = D_0(\xi_0/\xi_p)^\theta, \quad (3)$$

where

$$\xi_p = \xi_0[(p - p_c)/(1 - p_c)]^{-\nu_p}$$

and θ is the diffusion exponent.^{9,10} The low-frequency density of states is, therefore, given by (2). Short-wavelength excitations, however, must propagate along the (fractal) pathway provided by the dilute arrangement of exchange-coupled spins, and consequently obey a different dispersion law.⁴ The density of states for these excitations, which have been termed fractons in the analogous situation for lattice vibrations, has the form¹⁰

$$n_{fr}(\omega) \sim \omega^{\tau-1}, \quad (4)$$

where $\tau = 3/(2 + \theta)$ in three dimensions. This value for τ holds when the contribution of finite clusters is included in the calculation.¹¹ The crossover between the two regimes occurs⁷ at

$$\omega_c = D(p)(2\pi/\xi_p)^2 \sim \xi_p^{-(2+\theta)}. \quad (5)$$

In order to include possible fracton contributions to the temperature dependence of the magnetization, we introduce an effective DOS which interpolates between (2) and (4),

$$n_{eff}(\omega) = (1/4\pi^2)[\hbar/D(p)]^{3/2}\omega^{1/2}(1 + \omega/\omega_c)^{\tau-3/2}. \quad (6)$$

For large values of ω_c —the pure limit—we recover the normal density of states for spin waves. At the other extreme, density of states approaches the fracton limit with a coefficient that is independent of ξ_p . We use this density of states to fit the experimental data by treating $D(p)$ and ω_c as adjustable parameters at each concentration p . Correlations between θ and the other parameters prevent a simultaneous determination of all three. We fix θ and

search for self-consistency in the value of θ deduced from Eqs. (3) and (5). Consistency can be achieved only by fixing the exponent in the range $\theta = 1.5 \pm 0.1$, close to theoretical prediction.¹²

The magnetization is calculated by numerically integrating over the effective density of states, taking account² of the measuring field,

$$M(T) = M(0) - (g\mu_B) \int \frac{n_{\text{eff}}(\omega) d\omega}{\exp[(\hbar\omega + g\mu H)/k_B T] - 1} \quad (7)$$

The solid lines in Fig. 1 are fits of (7) to the data taken in an applied field of 10 kOe with $\mu = 1.6\mu_B$,¹³ and $\theta = 1.5$. Equation (7) assumes that all finite clusters are aligned with the applied field, and that all temperature dependence arises from the decrease in the moment of each cluster (and of the spontaneously magnetized infinite cluster) due to magnon and fracton excitations.

Values of $D(p)$ and $\omega_c(p)$ obtained from the fits in Fig. 1 are plotted versus reduced concentration in Fig. 2. The critical concentration $p_c = 0.325$ gives the best power-law fit to the data. The concentrations are nominal, but the transition temperatures are linear in $p - p_c$ above $p = 0.36$ as shown in Table I. Close to the percolation point, the determination of the transition temperature is complicated by spin-glass-like effects that are important at fields below 1 kOe. The data are well represented by the following power laws:

$$D(p) = D_0[(p - p_c)/(1 - p_c)]^{\theta\nu_p}, \quad (8)$$

with $\theta\nu_p = 1.3 \pm 0.1$ and $D_0 = 210 \pm 10 \text{ meV \AA}^2$, and

$$\omega_c(p) = \omega_0[(p - p_c)/(1 - p_c)]^{(2+\theta)\nu_p} \quad (9)$$

with $(2+\theta)\nu_p = 3.0 \pm 0.1$ and $\omega_0 = 1.6 \times 10^{14} \text{ s}^{-1}$. Note that these values of the exponents lead to $\nu_p = 0.85 \pm 0.07$

TABLE I. Properties of $(\text{Co}_p\text{Ni}_{1-p})_{75}\text{P}_{16}\text{B}_6\text{Al}_3$ samples used in this work. The last column shows that the Curie temperature is nearly linear in $p - p_c$.

Composition p (nominal)	Curie temperature (K)	$M(0)$ (G)	$T_c(1 - p_c)/(p - p_c)$ (K)
0.34	≈ 20	118	~ 900
0.36	38	120	732
0.38	53	140	650
0.40	84	160	757
0.50	175	245	676

and $\theta = 1.5 \pm 0.1$, both of which are consistent with theory¹² for three-dimensional site percolation and with our assumed value of θ . Equation (8) is very close to the numerical predictions of Ref. 8 for cubic lattices.

From the definition of ω_c it is straightforward to show that $\hbar\omega_0 = D_0(2\pi/\xi_0)^2$. Using the values of ω_0 and D_0 from the above fits, we estimate $\xi_0 \approx 9 \text{ \AA}$, which is the shortest distance over which the system can be regarded as fractal. This is approximately the diameter of the first shell of transition atoms surrounding a central transition atom, and is a reasonable value.

It must be pointed out that the analysis presented here is restricted to the low-temperature regime, since there is no Debye cutoff in (7). We have examined this by changing the upper limit in the numerical integration routine. The highest energy in the problem is $\hbar\omega_0 = 100 \text{ meV}$. The integral varied by less than 0.1% when the upper limit was reduced to half of this limiting energy. Of more serious concern is the form of the effective density of states, Eq. (6). A calculation based on the effective-medium approximation by Yu¹⁴ gave a step increase from the spin-

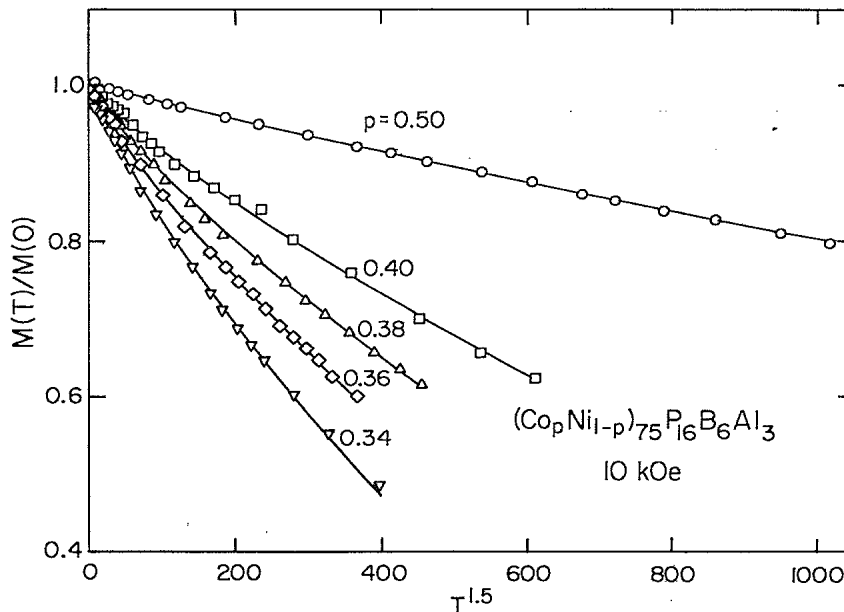


FIG. 1. Reduced magnetization vs temperature to the $\frac{3}{2}$ power. Upward curvature is anomalous. The solid lines are fits to the data using the spin-fracton-magnon density of states.

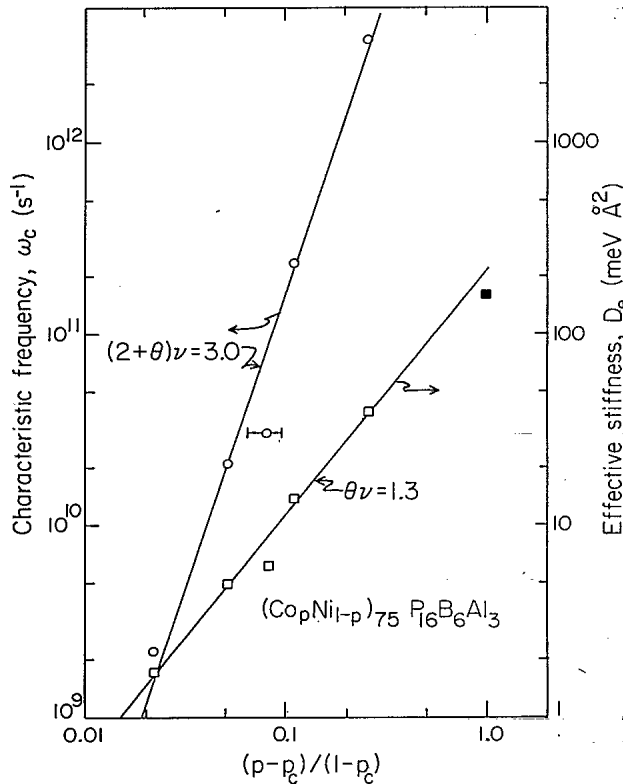


FIG. 2. Effective spin-wave stiffness $D(p)$ and magnon-fracton crossover frequency $\omega_c(p)$ vs reduced concentration. The critical concentration p_c is taken to be 0.325. The solid square is the pure limit value, from the normal Bloch law.

wave density of states (2) to the fracton density of states (4). Such a step would lead to a plateau in $M(T)$ in the vicinity of $T = \hbar\omega_c/k_B$; none is observed. The shape of the scaling function [the last factor in Eq. (6)] is less important in the magnon-fracton problem than it is in the phonon-fracton case. In the latter, the softening of the speed of sound and the quadratic phonon density of states cause a deficit in the density of states at low frequencies, leading to the conclusion⁷ that there must be a peak between phonon and fracton regimes. Here, because of the square-root density of states, Eq. (2), there is less of a deficit at low frequencies. The needed extra states can be accommodated by adjusting the Debye cutoff and do not demand an additional peak in the magnon-fracton density of states. Figure 3 shows the effective DOS functions actually used in the analysis; an alternative form, that follows (2) up to ω_c and then (4), gives identical results.

The present analysis resolves a number of long-standing problems in the magnetization of dilute ferromagnets. The stiffness constant $D(p)$ is now seen to vanish at the percolation point. The tendency toward a constant value reported previously,⁶ and the too-weak dependence on concentration¹⁵ were the result of the presence of fracton excitations. Close to the percolation point, the magnetization is dominated by the alignment of finite clusters, not

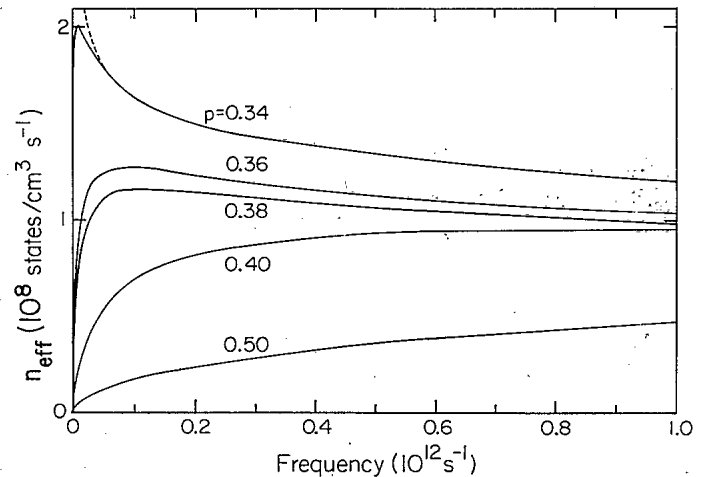


FIG. 3. The low-frequency region of the effective densities of states used in the fits shown in Figs. 1 and 2. The $p=0.34$ DOS is very close to the pure fracton limit (dashed curve).

by the very small true spontaneous moment. Therefore, even near the Curie point, the temperature dependence of the magnetization in a field is mainly governed by fracton excitations that disorder the clusters, rather than by the critical-point effects that disorder the spontaneous magnetization.

The broadening and downward shift of magnon peaks at low temperatures, observed by neutron scattering,^{16,17} remain unresolved problems. Aeppli, Shapiro, Birgeneau, and Chen¹⁷ have argued that random-field effects destroy long-range order, effectively making ξ_p temperature dependent. If so, then fracton effects would be more evident at low temperatures, but should cause the inelastic peaks to shift upward. It may be that the localized nature of fractons¹⁴ makes a determination of their frequency problematic.

In conclusion, an *ad hoc* magnon-fracton density of states consistently fits magnetization data for a series of magnetically dilute amorphous alloys and yields exponents that are in good agreement with percolation theory. The consistency of the picture lends support to the existence of fracton excitations in percolating magnets while resolving a number of anomalous features of magnetic behavior near the percolation point. It is likely that both the spin-wave stiffness constant D and the fracton dispersion are temperature dependent and would lead to a more rapid decrease of $M(T)$ at higher temperature. We have ignored this possibility and may, consequently, have underestimated the importance of fracton effects in dilute magnets.

This work was supported in part by the National Science Foundation Materials Research Laboratory Program through Grant No. NSF-DMR-83-16981, and in part by the Fund for Basic Research, administered by the Israel Academy of Science and Humanities.

- ¹F. Bloch, *Z. Phys.* **74**, 295 (1932).
- ²F. Keffer, in *Handbuch der Physik*, edited by S. Flugge (Springer, Berlin, 1966), Vol. 18, pp. 1-273.
- ³S. M. Bhagat, M. L. Spano, H. S. Chen, and K. V. Rao, *Solid State Commun.* **33**, 303 (1980).
- ⁴S. Alexander and R. Orbach, *J. Phys. (Paris) Lett.* **43**, L625 (1982).
- ⁵Y. J. Uemura and R. Birgeneau, *Phys. Rev. Lett.* **57**, 1947 (1986).
- ⁶Y. Yeshurun, K. V. Rao, M. B. Salamon, and H. S. Chen, *J. Appl. Phys.* **52**, 1747 (1981).
- ⁷A. Aharony, S. Alexander, O. Entin-Wohlman, and R. Orbach, *Phys. Rev. B* **31**, 2565 (1985).
- ⁸A. B. Harris and S. Kirkpatrick, *Phys. Rev. B* **16**, 542 (1977).
- ⁹Y. Gefen, A. Aharony, and S. Alexander, *Phys. Rev. Lett.* **50**, 77 (1983).
- ¹⁰D. ben Avraham and S. Havlin, *J. Phys. A* **15**, L69 (1982).
- ¹¹S. Alexander, C. Laermans, R. Orbach, and H. M. Rosenberg, *Phys. Rev. B* **28**, 4615 (1983).
- ¹²D. Stauffer, *Phys. Rep.* **54**, 1 (1979).
- ¹³K. Yamauchi and T. Mizoguchi, *J. Phys. Soc. Jpn.* **39**, 541 (1975).
- ¹⁴K. W. Yu, *Phys. Rev. B* **29**, 4065 (1984).
- ¹⁵L. S. Meichle and M. B. Salamon, *J. Appl. Phys.* **55**, 1817 (1984).
- ¹⁶J. W. Lynn, R. W. Erwin, H. S. Chen, and J. J. Rhyne, *Solid State Commun.* **46**, 317 (1983).
- ¹⁷G. Aeppli, S. M. Shapiro, R. J. Birgeneau, and H. S. Chen, *Phys. Rev. B* **29**, 2589 (1984).